

Supporting Information for

Screening of Red Phosphorus Supported Transition Metal Single-atom Catalysts for Efficient Photocatalytic Water Splitting H₂ Generation

Lu Lu,^[a] Mingzi Sun,^[a] Tong Wu,^[a] Qiuyang Lu,^[a] Baian Chen,^[a] Cheuk Hei Chan,^[a]
Hon Ho Wong,^[a] Bolong Huang*,^{[a][b]}

^[a]Department of Applied Biology and Chemical Technology, The Hong Kong Polytechnic University, Hung Hom, Kowloon, Hong Kong SAR, China

^[b]Research Centre for Carbon-Strategic Catalysis, The Hong Kong Polytechnic University, Hung Hom, Kowloon, Hong Kong SAR, China

*E-mail: bhuang@polyu.edu.hk (B. H.)

Calculation Setup

A comprehensive computational simulation has been taken on pristine red phosphorus (RP) and twenty-nine kinds of single-atom (SA) transition metal (TM) anchored TM-RP catalysts under density functional theory (DFT) with CASTEP code.¹ The GGA-PBE²⁻⁴ functional, LBFGS algorithm, and ultrasoft pseudopotentials have been set as basic computational parameters for all the geometry optimization and single-point energy calculation throughout the work. For the solution of the Kohn-Sham (KS) equation, we apply the ensemble DFT approach of Marzari et al. for the warranty of electronic minimization as well as convergence requirements.⁵ The cutoff energy in water adsorption (H_2O_{ad}) models has been set as 380 eV for pristine-RP and TM-RP. The k-point set is $2 \times 2 \times 1$ for all the energy minimizations, and the SCF tolerance is 5.0×10^{-7} eV/atom. The detailed convergence tolerance minimizer parameters have been indicated as follows: the energy tolerance is 5.0×10^{-6} eV/atom; the Max. Hellmann-Feynman force per atom is set as 0.01 eV/Å; the Max. stress is 0.02 GPa; and the Max. displacement is 5.0×10^{-4} Å. The RP (001) surface is cut from fully relaxed bulk Hittorf's phosphorus,⁶ with two monolayers containing 84 P atoms, resulting in a lattice parameter of 9.27 Å in length-A orientation and 9.21 Å in length-B orientation respectively. The vacuum thickness has been set as 20 Å, with a length of 40.95 Å obtained in C-orientation. The top view of pristine-RP and twenty-nine different kinds of TM atom anchored on RP (001) surfaces has been indicated in **Fig. S1**. During the H_2O_{ad} and H-adsorption (H_{ad}) process, the single-atom catalyst (SAC) surface has been constrained to focus on the key behaviors and adsorption properties of adsorbates. The H_{ad} energy (ΔE_H) has been calculated through the following equation^{7, 8}:

$$\Delta E_H = E_{H^*} - E^* - \frac{1}{2}E(H_2) \quad (1)$$

in which * represents the pristine RP surface without adsorption, and H^* indicates the surface adsorbed with H.

The Gibbs free energy change (ΔG_{H^*}) between the gas phase and the adsorbed state of hydrogen has been adopted as the descriptor for evaluating HER energy barriers. As proposed by Nørskov et al, ΔG_{H^*} can be calculated by the following equation:

$$\Delta G_{H^*} = \Delta E_{H^*} + \Delta E_{ZPE} - T\Delta S_H \quad (2)$$

in which ΔE_{H^*} indicates the chemisorption energy, ΔE_{ZPE} represents the zero point energy change, and ΔS_H represents the entropy change of H adsorption.⁷ The H-adsorption energies (ΔE_{H^*}) on different TM-RP facets are obtained via the following equation:

$$\Delta E_{H^*} = E_{(slab + H^*)} - E_{slab} - \frac{1}{2}E_{H_2} \quad (3)$$

where $E_{(slab + H^*)}$ means the total energy of the H-adsorption slab, E_{slab} indicates the energy of the pristine slab, and E_{H_2} represents the energy of H_2 . The zero point energy can be calculated as below:

$$\Delta E_{ZPE} = ZPE_{H^*} - \frac{1}{2}ZPE_{H_2} \quad (4)$$

in which ZPE_{H^*} and ZPE_{H_2} are zero-point energies of H in adsorbed and gas state, respectively. The reported value of ΔE_{ZPE} is 0.04 eV,⁷ and it has been considered as a reference value for all the TM-RP models calculated in this work. Since the vibrational

entropy of hydrogen in the adsorbed phase (S_{H^*}) is quite small, the ΔS_H can be calculated as follows:

$$\Delta S_H = S_{H^*} - \frac{1}{2}S_{H_2} \approx -\frac{1}{2}S_{H_2} \quad (5)$$

Herein, S_{H_2} stands for the entropy of hydrogen in the gas phase under standard state. At room temperature ($T = 298 \text{ K}$), the TS_{H_2} of gaseous H_2 is 0.41 eV ,⁹ and the $T\Delta S_H$ is calculated to be -0.204 eV .^{10, 11} As a result, ΔG_{H^*} can be calculated as:

$$\Delta G_{H^*} = \Delta E_{H^*} + 0.24 \text{ eV} \quad (6)$$

The formation energy (E_{Form}) values of TM-RPs can be calculated from the following Equation:

$$E_{\text{Form}} = E_{\text{TM-RP}} - E_{\text{TM}} - E_{\text{RP}} \quad (7)$$

in which the $E_{\text{TM-RP}}$ is the total energy of each TM-RP SAC model, E_{TM} is the energy of one SA-TM cut from the configuration of its corresponding SAC model, and E_{RP} is the total energy of the substrate RP surface.

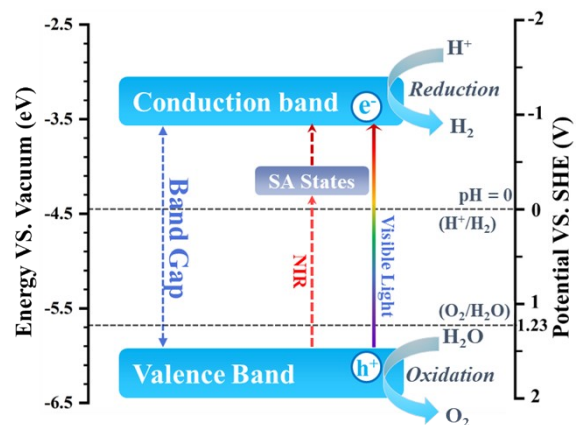


Figure S1. The schematic diagram of electronic modulation induced by the anchored SA-TMs.

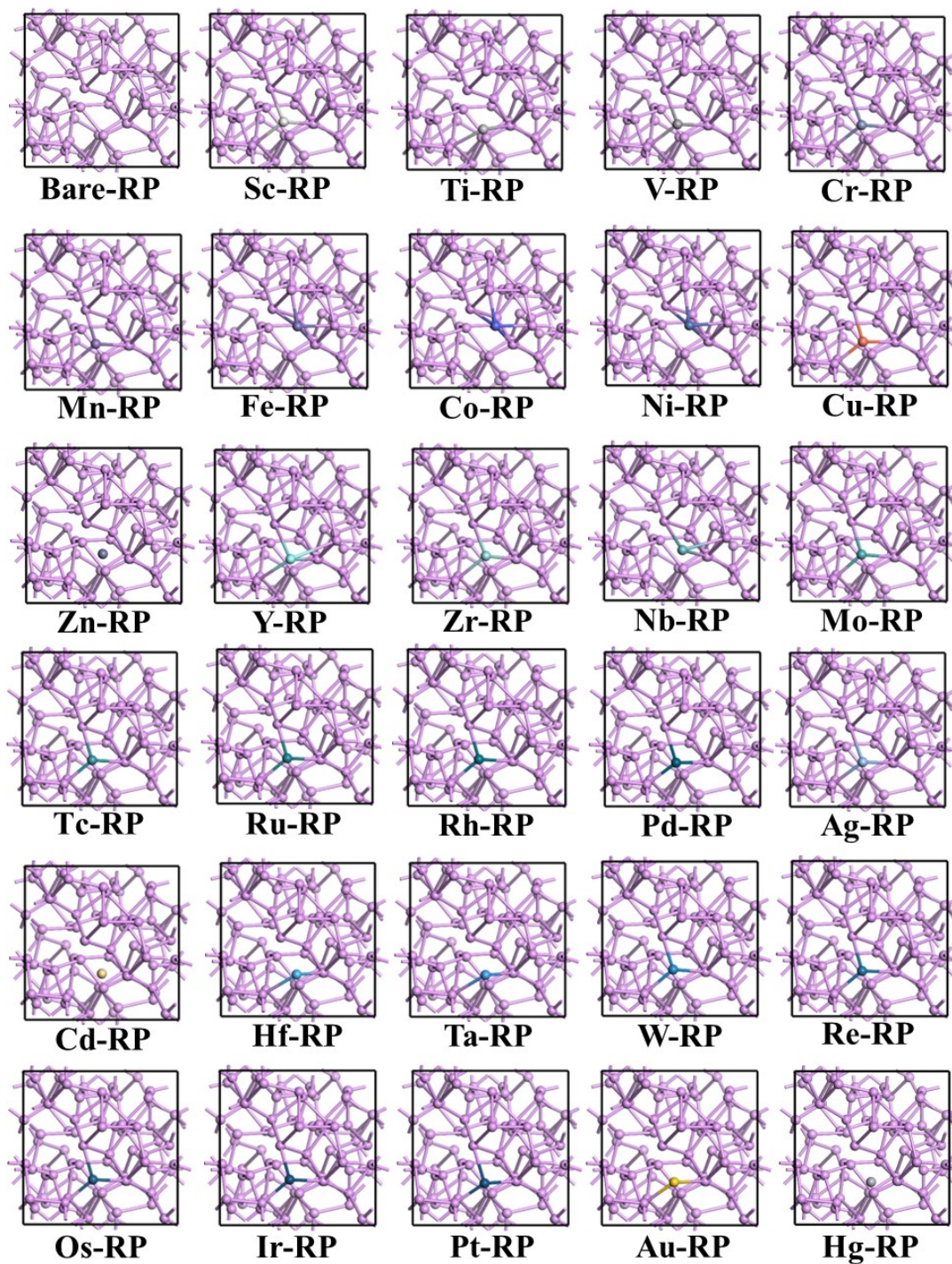


Figure S2. Configurations of pristine-RP and twenty-nine kinds of anchored active TM atoms on RP (001) surface.

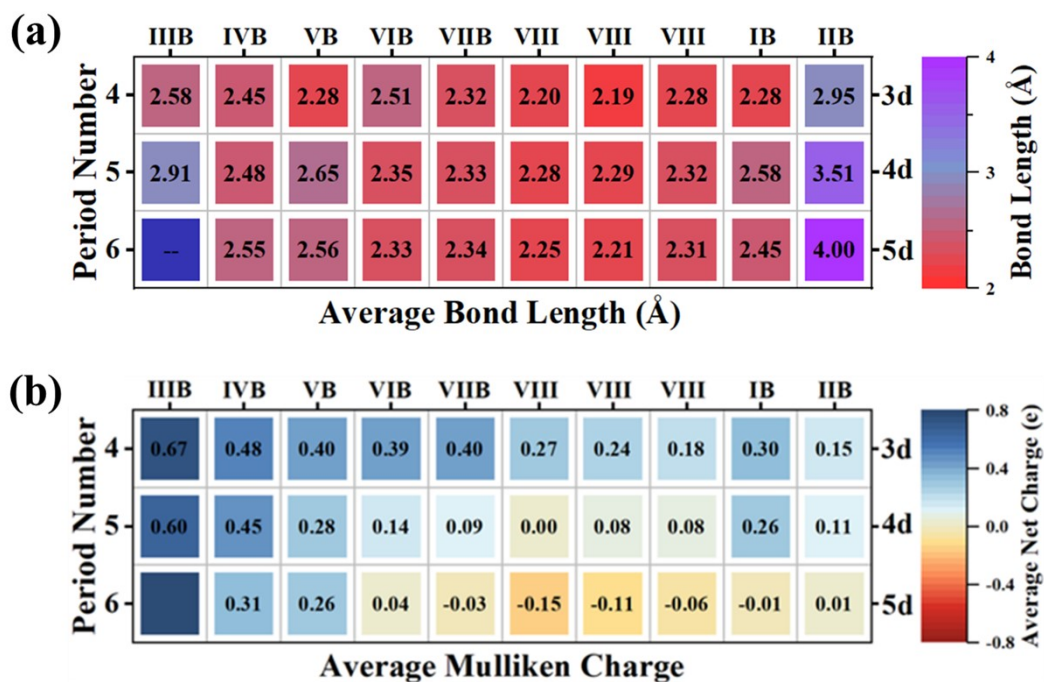


Figure S3. (a) The average bond length (TMs coordinated to surrounding P atoms) of twenty-nine active SA-TM atom types anchored on the RP (001) surface. (b) Mulliken charge analysis of twenty-nine active SA-TM atom types that anchored on RP (001) surface.

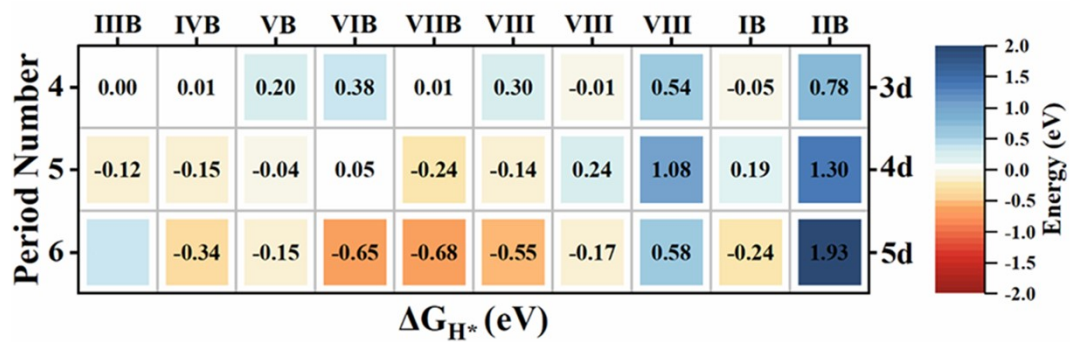


Figure S4. The mapping of ΔG_{H^*} for active TM sites for twenty-nine kinds of TM-RP SACs.

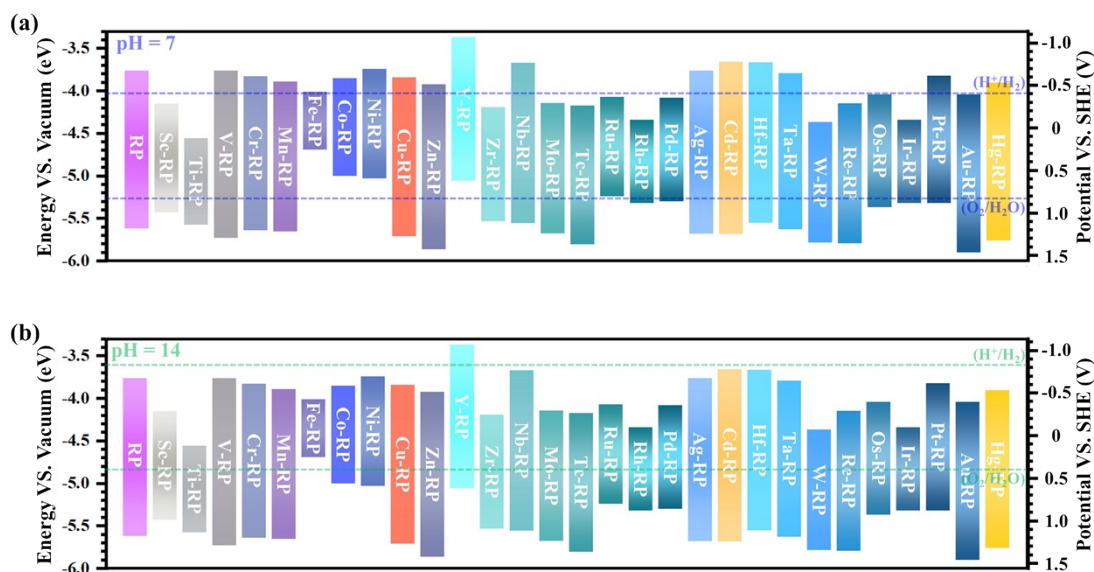


Figure S5. Band structure alignments in the scale of vacuum level (left) and SHE (right) for pristine-RP and twenty-nine types of TM-RP SACs. The blue and green dashed lines in the horizontal direction represent the redox potentials of water (H^+/H_2 and O_2/H_2O) at $pH = 7$ (a) and $pH = 14$ (b) respectively.

The pH change will alter the standard redox potentials of water based on Nernst equations:

$$E^{\text{HER}}(H^+/H_2) = -4.44 \text{ eV} + pH \times 0.059 \text{ eV} \quad (8)$$

$$E^{\text{OER}}(O_2/H_2O) = -5.67 \text{ eV} + pH \times 0.059 \text{ eV} \quad (9)$$

As a result, the photocatalytic reaction tendency for both HER and OER can be regulated via pH control. With the increase in pH, both the potential levels of H^+/H_2 and O_2/H_2O will move up, leading to a driving force decrease in HER and a corresponding increase in OER. That is, the HER and OER reaction tendency can be balanced for overall photocatalytic water splitting with the variation of pH. For instance, when $pH = 7$, the thermodynamic HER and OER driving force of pristine-RP, V-RP, Cr-RP, Nb-RP, Ag-RP, Cd-RP, Hf-RP, and Ta-RP are in similar values, exhibiting their great potential for overall water splitting at neutral condition. While in the highly alkaline conditions ($pH = 14$), except Y-RP and La-RP, pristine-RP and most TM-RP SAC candidates will lose their HER capacity from the perspective of thermodynamics.

References

1. S. J. Clark, M. D. Segall, C. J. Pickard, P. J. Hasnip, M. I. J. Probert, K. Refson and M. C. Payne, *Zeitschrift für Kristallographie - Crystalline Materials*, 2005, **220**, 567-570.
2. J. P. Perdew, K. Burke and M. Ernzerhof, *Phys. Rev. Lett.*, 1996, **77**, 3865-3868.
3. P. J. Hasnip and C. J. Pickard, *Computer Physics Communications*, 2006, **174**, 24-29.
4. J. P. Perdew, J. A. Chevary, S. H. Vosko, K. A. Jackson, M. R. Pederson, D. J. Singh and C. Fiolhais, *Physical Review B*, 1992, **46**, 6671-6687.
5. N. Marzari, D. Vanderbilt and M. C. Payne, *Physical Review Letters*, 1997, **79**, 1337-1340.
6. H. Thurn and H. Krebs, *Angewandte Chemie*, 1966, **78**, 1101-1102.
7. J. K. Nørskov, T. Bligaard, A. Logadottir, J. R. Kitchin, J. G. Chen, S. Pandalov and U. Stimming, *Journal of The Electrochemical Society*, 2005, **152**, J23-J26.
8. U. Kerketta, A. B. Tesler and P. Schmuki, *Catalysts*, 2022, **12**, 1223.
9. Y. Liu, G. Yu, G.-D. Li, Y. Sun, T. Asefa, W. Chen and X. Zou, *Angewandte Chemie International Edition*, 2015, **54**, 10752-10757.
10. N. N. T. Pham, S. G. Kang, H.-J. Kim, C. Pak, B. Han and S. G. Lee, *Applied Surface Science*, 2021, **537**, 147894.
11. Z. Liang, X. Zhong, T. Li, M. Chen and G. Feng, *ChemElectroChem*, 2019, **6**, 260-267.